Available online at www.sciencedirect.com

SCIENCE DIRECT

Powder Technology 154 (2005) 164 – 178

POWDER TECHNOLOGY

www.elsevier.com/locate/powtec

Multi-Monte Carlo approach for general dynamic equation considering simultaneous particle coagulation and breakage

Zhao Haibo*, Zheng Chuguang, Xu Minghou

State Key Laboratory of Coal Combustion, Huazhong University of Science and Technology, Wuhan 430074, People's Republic of China

Received 28 November 2004; received in revised form 8 March 2005; accepted 21 April 2005
Available online 14 June 2005

Abstract

Particle size distribution is described by general dynamic equation (GDE). A new multi-Monte Carlo (MMC) method is promoted to solve GDE for simultaneous particle coagulation and breakage. MMC method is based on "time-driven" Monte Carlo technique and conserves constant number of fictitious particles and constant volume of computational domain with the evolution of time. Firstly, MMC method is described in details, which includes the scheme of simultaneous coagulation and breakage, the introduction of "weighted fictitious particle", the setting of time step, the judgment of the occurrence of coagulation and breakage event, the choice of fictitious coagulation partner, and dealing with the consequence of particle coagulation and breakage event. Then MMC method is used to simulate four kinds of special cases in which complete or partial analytical solutions exist; the simulation results of MMC method for GDE agree with analytical solutions well, which proves that MMC method has high and stable statistical precision.

Keywords: Population balance; Numerical solution; Particle size distribution; Computation cost; Computation precision; Kernel

1. Introduction

Coagulation and breakage take effect in many nature fields and engineering courses, including formation and evolvement of air aerosols and emulsion droplets, and manufacture of nanoparticle agglomerates, etc. For example, coagulation and breakage of pulverized coal fly ash during combustion are main mechanisms of the formation of particulate matter (PM) [1,2]; coagulation and breakage occur simultaneously for long chain polymer in chemical engineering and fine droplets in spray flow or spray combustion, leading to an equilibrium distribution. Because many important properties of particles (for example, light scattering, electrostatic charging, toxicity, radioactivity, sediment and capturing strategy, etc.) depend on their size distribution, the time evolution of size distribution is of fundamental interest and key issue [3].

Particle size distribution (PSD) along with time is described by general dynamic equation (GDE), which can take account of physical and chemical processes such as coagulation, condensation/evaporation, nucleation, breakage and deposition, etc. GDE for simultaneous particle coagulation and breakage is as follows [4]:

$$\frac{dn_p(v,t)}{dt} = \left\{ \int_v^{v_{max}} \gamma(u,v)b(u)S(u)n_p(u,t)du - S(v)n_p(v,t) \right\}_{breakage} + \left\{ \frac{1}{2}\int_{v_{min}}^{v} \beta(v-u,u)n_p(v-u,t)n_p(u,t)du - n_p(v,t)\int_{v_{min}}^{v_{max}} \beta(v,u)n_p(u,t)du \right\}_{coagulation} \quad (1)$$

where $n_p(v,t)$ is particle size distribution function at time t, says, $n_p(v,t)dv$ is the number of particles whose size range

* Corresponding author. Tel.: +86 27 8754 4779x8318; fax: +86 27 8754 5526.
E-mail address: klinsmannzhb@163.com (Z. Haibo).

0032-5910/$ - see front matter © 2005 Elsevier B.V. All rights reserved.
doi:10.1016/j.powtec.2005.04.042

between v and $v+dv$ per volume unit at time t; the dimension of $n_p(v,t)$ is particles m^{-3} m^{-3}, where "particles" denotes the number of particles; $\beta(v,u)$ is coagulation kernel for two particles of volume v and u, m^3 particles^{-1} s^{-1}. $S(v)$ is breakage rate for particle of volume v, with dimension s^{-1}; $\gamma(u,v)$ is the probability of making a daughter of volume v from a parent of volume u, $b(u)$ is the number of particles resulting from the breakage of a particle of volume u. $\gamma(u,v)b(u)$ describes size distribution of particle of volume u resulting from the breakup of a particle of volume v. The term on the left-hand of Eq. (1) describes the change in number concentration of particle of volume v with time; the two terms on the right-hand describe the gain and loss in number concentration respectively due to breakage and coagulation. The first part in the "breakage" term on the right-hand of Eq. (1) describes the breakage of particle of volume u bigger than particle of volume v to yield particle of volume v, and the second part represents the breakage of particle of volume v with a statistical probability of $S(v)$. The first part in the "coagulation" term accounts for the formation of particle of volume v, and the second part shows the disappearance of particle of volume v due to coagulation with any particle.

Particle size distribution is usually polydisperse and spans widely, for example, pulverized coal fly ash particle formation is accurately described as a tri-modal PSD that includes a submicron fume region centered at approximately 0.08 μm diameter, a fine fragmentation region centered at approximately 2.0 μm diameter, and a bulk or supermicron fragmentation region for particles of approximately 5 μm diameter and greater [1]; and then, GDE is a typical partially integro-differential equation; In addition, some kinds of mechanisms such as coagulation and breakage impose different, complicated and nonlinear effects on PSD. The above factors result in numerical predicament where normal numerical methods (such as finite element method and finite difference method, etc.) can hardly take account of GDE. Nowadays the most popular numerical methods for GDE are moments of method [5], Monte Carlo method [6–13], sectional method [14], discrete method [15] and discrete–sectional method [16], etc. Those methods have both advantage and disadvantage.

The merit of moments of method is little computation time and simple mathematical representations, however the model need assume initial special-shaped particle size distribution, or monodisperse, or self-preserving, or the employed Taylor expansion; in addition there is no information about the history of each particle which collides to form a bigger particle.

Sectional method approximates the continuous PSD by a finite number of sections within which the PSD function is assumed to be constant. The model has receivable computation cost and computation precision by the selection of the proper number of sections employed and the numerically conserved integral property of the PSD. However, sectional representation results in complex algorithms, and has bad numerical accuracy on the lower end of PSD. Furthermore it is troublesome for the method to handle multi-component, more-dimensional, chemical reaction and coating, etc.

Discrete method solves the detailed general dynamic equation and therefore most accurately describe the time evolution of PSD. Discrete model can be used for validation of other approximate GDE algorithm or for investigation of the attainment of asymptotic self-preserving PSD. However the model requires tremendous amounts of CPU time and computer memory, which constraints mostly its engineering application.

Discrete–sectional method is a combination of discrete method and sectional method. The method utilizes discrete method with finite number of bins to describe the lower end of PSD (discrete size region) and sectional method with proper number of sections to account for the other part of PSD (sectional size regime). The method makes full use of some advantages of discrete method and sectional method, at the same time overcomes properly some disadvantages of two parent methods. So discrete–sectional method has satisfying accuracy and speed. However the combination of discrete method and sectional method results in more complicated mathematical representations and more computation cost than sectional method.

As far as Monte Carlo (MC) method is considered, it can gain information about history, trajectory crossing and internal structure of particles; the Monte Carlo algorithms for solving polydisperse and multi-component GDE are easily programmed even considering restructuring, coating, chemical reaction and fractal aggregation [13]. The disadvantage of Monte Carlo method is time-consuming comparatively, and there is contradiction between computation cost and computation precision when normal MC method is used to consider coagulation and breakage, which will be explained in the following text. Along with more and more strong computer power, simulation with some 10^4 to 10^7 particles is possible on fast PCs, which relieves greatly the contradiction of expensive computation. In a word, Monte Carlo method is an attractive way of solving GDE because its discrete nature adapts itself naturally to the being modeled mechanisms coagulation and breakage, which involve discrete events.

Many researchers have investigated Monte Carlo method for solving GDE. Summing up, MC method can be divided into two classes according to the approach of time-step setting: one is referred to as "time-driven" Monte Carlo [17], which takes account of any possible event within an adjustable time-step. Here time-step must be less than or equal to the minimum time within which every possible event takes place once at most for every simulation particle. "Time-driven" MC need divide explicitly time window into intervals, and it's possible for one simulation particle that no any event is examined within one interval, which will cost significant amounts of simulation time; the other is called "event-driven" Monte Carlo [18]. In general special events are implemented stochastically with probabilities derived from mean-field rates of corresponding process. In simu-

lation of event-driven MC, a single event is selected to occur, and time is advanced by an appropriate increment. In contrast to time-driven MC, this MC doesn't need explicit time discretization and its time step, which is calculated during simulation, adjusts itself to rates of various event processes. However, one approach of "event-driven" MC, inverse method [18], need compute total coagulation rate with a double circle over $N(N-1)/2$ pairs or total breakage rate with a single circle over N pairs (where N is the number of simulation particles) after each coagulation or breakage event, which is time-consuming if N is large. As for the other approach of "event-driven" MC, acceptance–rejection method [18], if the range of PSD spans widely, the ratio of the randomly generated coagulation kernel (or the randomly generated breakage kernel) and the maximum coagulation kernel (or the maximum breakage kernel) becomes very small, which will slow down program considerably because of the large number of rejections. Furthermore acceptance–rejection method is an approximate solution, which has a rather large error when long time evolution [13].

On the other hand, MC method can also be classified into two general classes according to whether or not the total number of simulation particles and simulation domain are changed during MC simulation. The first approach is to track a constant volume and thus grow or shrink the total number of simulation particles in direct proportion to number concentration of physical system, while conserving mass. This method is sometimes referred to as "constant-volume MC", which can't maintain constant statistical accuracy because the total number of simulation particles continues to fluctuate. When coagulation is considered, the total number of real particles continues to decrease, so does the total number of simulation particles in constant-volume MC. At the time the initial number of simulation particles must be set to be enough large in order to satisfy proper computation precision, which will burden computation cost more badly. On the contrary, the total number of simulation particles will continue to increase when particle breaks up, which will also aggravate computation time. So there is the contradiction between computation cost and computation precision in constant-volume MC. The second class is "constant-number MC" promoted by Matsoukas and colleagues [10–12], in which simulation volume is continuously adjusted so as to contain constant number of simulation particles. The constant-number method maintains constant statistical accuracy and can simulate growth over arbitrarily long times with a finite number of simulation particles. Nevertheless, contraction or expansion of simulation volume results in bad applicability in engineering computation and general scientific quantitative analysis. Other similar constant-number methods, direct simulation algorithm [19–21] or mass flow algorithm [22–24], have been examined and reviewed by Ref. [25].

As for simultaneous particle coagulation and breakage, the occurrence of coagulation event decreases the total number of real particles; on the contrary, the occurrence of breakage event increases the total number of real particles. The competition between coagulation and breakage makes the total number of real particles fluctuate sharply, which embarrasses greatly the implement and maneuverability of Monte Carlo method. We have developed a new multi-Monte Carlo (MMC) method for coagulation [26] and simultaneous coagulation and condensation/evaporation [27]. MMC method has characteristics of time-driven, constant-number and constant-volume MC technique. Those technique are integrated a whole, which is named as multi-Monte Carlo (MMC) method. The paper tries to perform MMC method to consider GDE for simultaneous coagulation and breakage. Firstly the scheme and framework of MMC method for simultaneous coagulation and breakage are described in details. Then some numerical simulations of special cases are made using MMC method for GDE, and the comparison of simulation results with corresponding analytical solutions is taken.

2. Description for multi-Monte Carlo method

2.1. Designing the scheme of multi-Monte Carlo method for simultaneous coagulation and breakage

The new MC method is designed as "time-driven" MC technique, says, every simulate particle is tracked, and both possible binary coagulation event and possible breakage event are considered within time step Δt. The method introduces the concept of "weighted fictitious particle", which will be described in detail in Section 2.2. Although the total number of real particles fluctuates continuously along with the occurrence of coagulation event and breakage event, the total number fictitious particles keeps constant by means of the adjustment of the weight of those related fictitious particles. In addition, the volume of computational domain is conserved. Those technical details will be shown in Sections 2.4 and 2.5. In MMC method, particle coagulation event and breakage event can be decoupled within a sufficiently small time step Δt, that is, the evolution is decomposed into two distinct processes: coagulation event and breakage event. The scheme of MMC method for simultaneous coagulation and breakage is shown in Fig. 1.

Within one time step, the dynamic events of one particle are uncoupled with each other, that is, the particle may coagulate, or break up, or both coagulate and break up, or neither coagulation nor break up. Coagulation event is independent of breakage event in the same circle over all fictitious particles. It was also noticeable that the dynamic evolution of one particle is uncoupled with that of other particles, that is, every particle has probability of the occurrence of dynamic events. So in MMC method, within one time step there may be many coagulation events and many breakage events. Of course null event is possible if

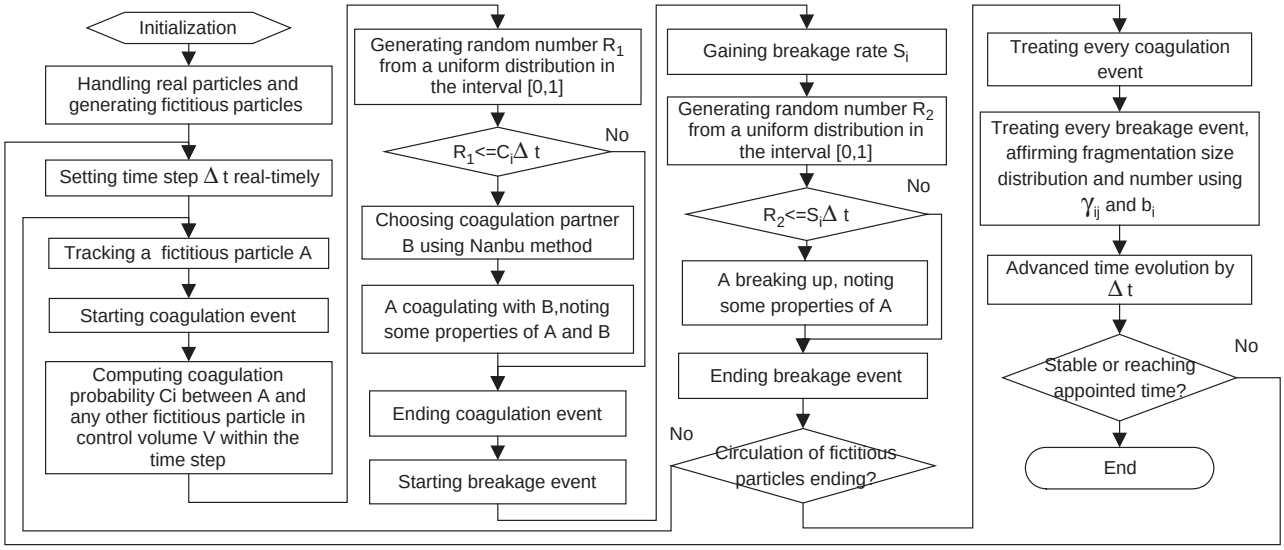

Fig. 1. The scheme of Multi-Monte Carlo method for simultaneous coagulation and breakage.

the coagulation probability of particle or the breakage probability of particle is enough small.

It is noticeable that coagulation and breakage event do not change immediately properties and behaviors of the tracked fictitious particle and the interrelated fictitious particles within current time step. The effects of coagulation and breakage event will be taken in the next time step. So dealing with the consequence of particle coagulation and breakage event should be delayed until the end of current time step, which can refer to Fig. 1.

The key points of MMC method include transforming real particles into fictitious particles, setting time step real-timely, judging whether or not coagulation and breakage event occur, choosing fictitious coagulation partner, and dealing with the consequence of particle coagulation and breakage event, which are described in detail in the following text.

2.2. Transforming real particles into fictitious particles

Because of the limit of computation capacity of PCs, Monte Carlo code can only examine $10^4 \sim 10^7$ particles at a time. However, a reasonably sized system of dispersed system contains approximately 10^7 or even more particles. So in known Monte Carlo methods [6–13,17–24] a subsystem of the total system is considered either implicitly or explicitly. "Subsystem" contains $10^3 \sim 10^7$ simulation particles, as each simulation particle represents some real particles, says, each simulation particle has a number-weight. Ones assume the whole system is fully-stirred and spatially isotropic, and the subsystem satisfies the constraint of periodic boundary conditions, i.e., as some particles move out from one boundary of the subsystem, some identical particles move in from the symmetrical boundary of the subsystem. By those hypotheses the behavior of the subsystem duplicates the system as a whole. "Subsystem" hypothesis makes it difficult for those Monte Carlo methods to simulate the whole system and to consider space dispersion of particle size function, boundary conditions and particle Lagrangian tracking, which is important in coupling with two-phase Euler/Lagrange model to investigate particle-flow interaction and particle dynamics.

The number-weight in constant-volume MC is same for all particles and constant during simulation. As far as constant-number MC [10–12] is considered, in the cases of breakage and nucleation that result in net generation of real particles, the volume of "subsystem" is contracted in order to maintain constant number of simulation particles; with mechanisms such as coagulation and deposition which make for net depletion of real particles, this amounts to the expansion of the simulated "subsystem". Factually the number-weight in constant-number MC is same for all particles but varies synchronously and unisonantly.

Different from the above approaches, MMC method introduces the concept of "weighted fictitious particle" in order to conserve the volume of computational domain and the number of fictitious particles within computational domain. One believes that those real particles that have same or similar volume can be considered to have same properties and hence same behaviors. Those real particles can be represented by one or several weighted fictitious particles, where fictitious particles are an indicator of those real particles. If the weight of one fictitious particle is "kwt", the fictitious particle represents "kwt" real particles. So the time evolution of fictitious particle duplicates that of real particle.

Fig. 2 shows schematic representation of relation between real particle and fictitious particle system. As shown in Fig. 2, every class of real particle population is represented by some fictitious particles, and the volume of

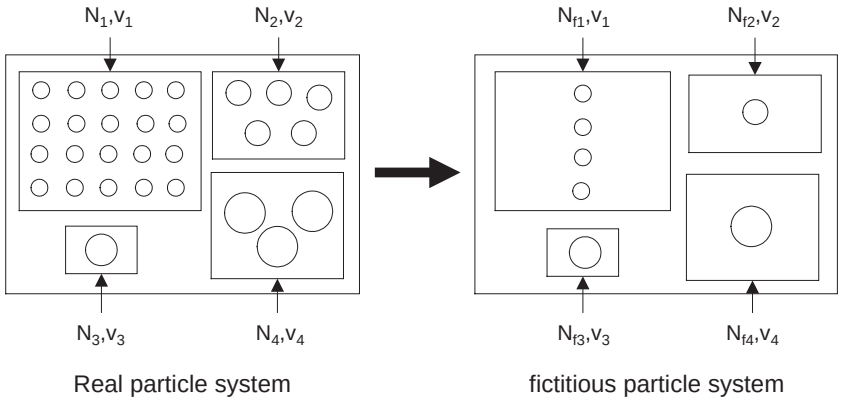

Fig. 2. Schematic representation of relation between real particle and fictitious particle system.

fictitious particles is just the volume of those represented real particles.

Fig. 3 shows the pictorial representation of numerical selection of transform-weight "kwt" of fictitious particle. Bin discretization of real particle size distribution is taken firstly, and then every class of real particle population is represented by some fictitious particles. Those fictitious particles of the same class have same value of transform-weight "kwt", however different value for different class. Generally speaking, MMC method still maintains high computation precision even though the value of "kwt" reaches to the magnitude of $O(10^3)\sim O(10^4)$. In fact, one fictitious particle can be seen as one bin of real particle size distribution, and particles in a given size range are represented by a bin that contains "kwt" real particles. Since Monte Carlo approach tracks discrete *particles* instead of *bin* in normal description, the nomenclature of "fictitious particle" instead of "bin" is used. A factual example is shown in Ref. [27].

During simulation, every fictitious particle is tracked. According to different consequence of different events, the transform-weight "kwt" and the volume of those related fictitious particles are changed, instead both computational domain and the number of fictitious particles are maintained during the time evolution of system. In fact, only those fictitious particles which coagulate or break up vary their "kwt" and volume with time in MMC method, and those changes depend on factual event, neither synchronously nor unisonantly, which will be described in detail in Sections 2.4 and 2.5.

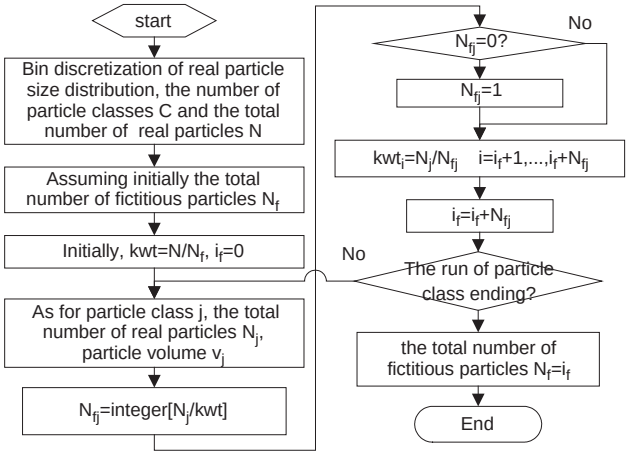

Fig. 3. Numerical selection of transform-weight of fictitious particle.

Since a smaller number of fictitious particles are evolved circularly in MMC method (seen in Fig. 1), computation cost will decrease accordingly, especially when the total number of real particles is very large within computational domain. Furthermore, the introduction of "weighted fictitious particle" makes it possible to discard the introduction of "subsystem". For example, if the total number of real particles in the whole system is small or one fictitious particle is permitted to represent more real particles at a cost of lower computation precision, the total number of fictitious particles could be within the scope of computer ability. Under the circumstances MMC method can discard "subsystem" concept and then has expansibility to consider the space evolution of PSD, boundary conditions and even gas-particle dynamics by means of coupling with two-phase turbulent model and plotting grid, etc. Of course, the total number of fictitious particles is still a large magnitude for the total system having a large number of real particles, when "subsystem" concept must be continued to use in MMC method.

2.3. Setting time step

In time-driven MC, every possible event should be considered within time step Δt. So the number of coagulation event of every fictitious particle must be less than or equal to one within Δt, and the number of breakage event of every fictitious particle must also be less than or equal to one within Δt.

Firstly we investigate the constraint of time step due to the occurrence of coagulation event. Ones can consider fictitious particle as one group of real particles. Thus the number of coagulation events occurring among ith-group (where those real particles are represented by fictitious particle i, and number concentrations per unit volume is kwt_i) and jth-group particles (fictitious particle j, number

concentrations per unit volume kwt_j) per unit time per unit volume is given by

$$NC_{ij} = \beta_{ij} \times \mathrm{kwt}_i \times \mathrm{kwt}_j \tag{2}$$

where β_{ij} is coagulation kernel for particle i and j, which represents the probability of a binary coagulation event per unit time.

For like particles, the number of coagulation events per unit time per unit volume is taken as [28]:

$$NC_{ii} = \beta_{ii} \times \mathrm{kwt}_i \times (\mathrm{kwt}_i - 1)/2. \tag{3}$$

If one assumes the total number of real particles is N and fictitious particles N_f, then NC_i, the total number of coagulation events of fictitious particle i per unit time per unit volume, is as follows:

$$NC_i = \sum_{j=1,\, j\neq i}^{N_\mathrm{f}} NC_{ij} + NC_{ii} = \sum_{j=1,j\neq i}^{N_\mathrm{f}} \left(\beta_{ij} \times \mathrm{kwt}_i \times \mathrm{kwt}_j\right) + \beta_{ii} \times \mathrm{kwt}_i \times \frac{(\mathrm{kwt}_i - 1)}{2}. \tag{4}$$

Since fictitious particle i represent kwt_i real particles, the average number of coagulation events of each real particle with any real particle per unit time is followed as:

$$nc_i = NC_i/\mathrm{kwt}_i = \sum_{j=1,\, j\neq i}^{N_\mathrm{f}} \left(\beta_{ij} \times \mathrm{kwt}_j\right) + \beta_{ii} \times \frac{(\mathrm{kwt}_i - 1)}{2}. \tag{5}$$

Since fictitious particle i is an indicator of those represented real particles, C_i, the total coagulation probability of fictitious particle i, is as follows:

$$C_i = nc_i = \sum_{j=1,i\neq j}^{N_\mathrm{f}} \left(\beta_{ij} \times \mathrm{kwt}_j\right) + \frac{\beta_{ii} \times (\mathrm{kwt}_i - 1)}{2}. \tag{6}$$

Then, coagulation time scale of fictitious particle i, within which only one coagulation event occurs, is as follows:

$$t_{i,\mathrm{coag}} = \frac{1}{C_i}. \tag{7}$$

Likewise, breakage time scale of fictitious particle i, within which only one breakage event occurs, is

$$t_{i,\mathrm{brk}} = \frac{1}{S_i}, \tag{8}$$

where S_i is breakage rate of fictitious particle i, which represents probability of breakage of fictitious particle i in unit time.

In MMC method, time step Δt should be less than or equal to the minimum coagulation time scale ($\min(t_{i,\mathrm{coag}})$), and also be less than or equal to the minimum breakage time($\min(t_{i,\mathrm{brk}})$), that is:

$$\Delta t \leq \min\left\{\frac{1}{\max_{i=1,\ldots,N_\mathrm{f}}(C_i)}, \frac{1}{\max_{i=1,\ldots,N_\mathrm{f}}(S_i)}\right\}. \tag{9}$$

MC is a stochastic approach, computational precision of which depends on the total number of simulation particles and the number of MC loop. In order to increase the number of Monte Carlo loop, time step is usually defined as

$$\Delta t = \alpha \min\left\{\frac{1}{\max_{i=1,\ldots,N_\mathrm{f}}(C_i)}, \frac{1}{\max_{i=1,\ldots,N_\mathrm{f}}(S_i)}\right\}. \tag{10}$$

The multiplicative constant, α, has the value of 0.01 or less. As coagulation kernel is unbounded, the smallest time scale is unusually due to coagulation. So during numerical simulation time step Δt is factually defined as

$$\Delta t = \frac{\alpha}{\max_{i=1,\ldots,N_\mathrm{f}}(C_i)}. \tag{11}$$

2.4. Treating particle coagulation event

Treating particle coagulation includes the judgment of the occurrence of coagulation event, the choice of coagulation partner, and dealing with the consequence of coagulation event.

The Nanbu method [29] is used to judge the occurrence of coagulation event and to choose coagulation partner. A schematic diagram (Fig. 4) is used to give readers a quantitative image of Nanbu method.

A random number R_1 from a uniform distribution in the interval [0,1] is generated. A coagulation event of the tracked fictitious particle i is calculated when the random number R_1 becomes smaller than the coagulation probability of i within Δt, i.e. if

$$R_1 \leq C_i \times \Delta t. \tag{12}$$

Once coagulation event occurs, the next issue is choosing coagulation partner of the tracked fictitious particle i.

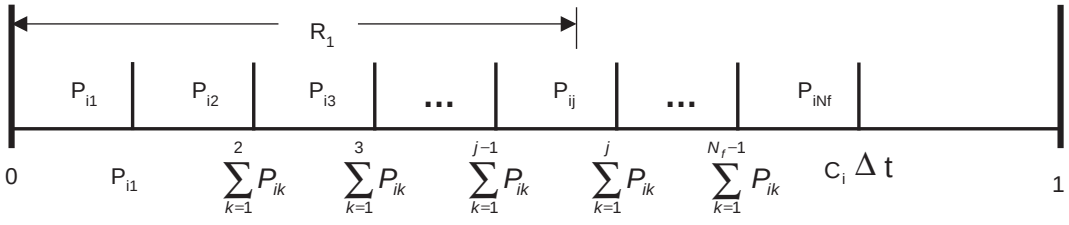

Fig. 4. The schematic diagram of Nanbu method.

Firstly, the probability of particle i coagulating with any other fictitious particles j is expressed as

$$P_{ij} = \mathrm{kwt}_j \times \beta_{ij} \times \Delta t. \tag{13}$$

And coagulation probability among the same fictitious particle i is expressed as

$$P_{ii} = [(\mathrm{kwt}_i - 1)/2] \times \beta_{ii} \times \Delta t \tag{14}$$

Obviously,

$$C_i \times \Delta t = \left[\sum_{j=1, i\neq j}^{N_f} \left(\beta_{ij} \times \mathrm{kwt}_i\right) + \frac{\beta_{ii} \times (\mathrm{kwt}_i - 1)}{2} \right] \times \Delta t = \sum_{k=1}^{N_f} P_{ik}. \tag{15}$$

Secondly the same random number R_1 is used for the determination of true coagulation partner. If the relation

$$\sum_{k=1}^{j-1} P_{ik} \leq R_1 \leq \sum_{k=1}^{j} P_{ik} \qquad j \in [1, N_f]. \tag{16}$$

is satisfied, it is decided that the tracked particle i coagulate with fictitious particle j. If not, the second step is repeated until the true coagulation partner is found out.

The direct result of particle coagulation is that two smaller real particles disappear and instead one bigger real particle produces. Along with the occurrence of particle coagulation event, the total number of simulation particles cuts down continuously in ordinary constant volume Monte Carlo method. If the number of sample space decreases continuously, computation precision of Monte Carlo method will decrease accordingly. One of important points of MMC method is to keep the total number of fictitious particles constant.

Every fictitious particle represents some real particles. When the tracked fictitious particle "A" coagulates, it means some real particles represented by "A" (its number concentration is $\mathrm{kwt_A}$, its volume is v_A) coagulate. Likewise, when the tracked fictitious particle "B" coagulates, it implies some real particles represented by "B" (its number density is $\mathrm{kwt_B}$, its volume is v_B) coagulate. Because the "A" is a signal of some real particles, ones can neglect the factual progress of the coagulation event, that is, it is insignificant to know which coagulate with their partner, or to differentiate whether or not the number of real particles represented by "A" is equal to the number of real particles represented by "B". Instead ones should focus on the direct result of coagulation event. As a direct result of coagulation event, those "old" real particles represented by A and B are changed as bigger real particles, and the total number of those bigger real particles is the half of the total number of those "old" real particles.

In order to keep the total number of fictitious particles constant, both the tracked fictitious particle and its partner are conserved. Accordingly their transform-weight kwt and their volume are adjusted to satisfy the law of conservation of mass and the rule of change of number. It is considered that the transform-weight of both the tracked fictitious particle A and its partner B are halved, respectively, and the volume of both A and B is changed as $v_A + v_B$. Because one coagulation event of particle pairs is double-counted within each time step Δt, only some properties of the tracked fictitious particle are changed, where no any change is made in its partner. The strategy of the consequential treatment of coagulation event is shown in Fig. 5. It is noticeable that transform-weight kwt is not always integer, although every kwt in Fig. 5 is endowed with integer for the purpose of convenient plotting. When the tracked fictitious particle is "A", the following measures are taken:

$$(\mathrm{kwt_A})_{\mathrm{new}} = \mathrm{kwt_A}/2; (v_A)_{\mathrm{new}} = v_A + v_B. \tag{17}$$

When the tracked fictitious particle is assigned to "B" in turn, its coagulation partner will be "A" theoretically and the same measure is taken:

$$(\mathrm{kwt_B})_{\mathrm{new}} = \mathrm{kwt_B}/2; (v_B)_{\mathrm{new}} = v_A + v_B. \tag{18}$$

The measures not only conserve the number of fictitious particles but also accord with the reality of coagulation event, no matter how many coagulation events there are and how long the evolution time is.

2.5. Treating particle breakage event

Treating particle breakage includes the judgment of the occurrence of breakage event and dealing with the consequence of breakage event.

R_2 is a random number from a uniform distribution in the interval [0,1]. A breakage event of fictitious particle i occurs

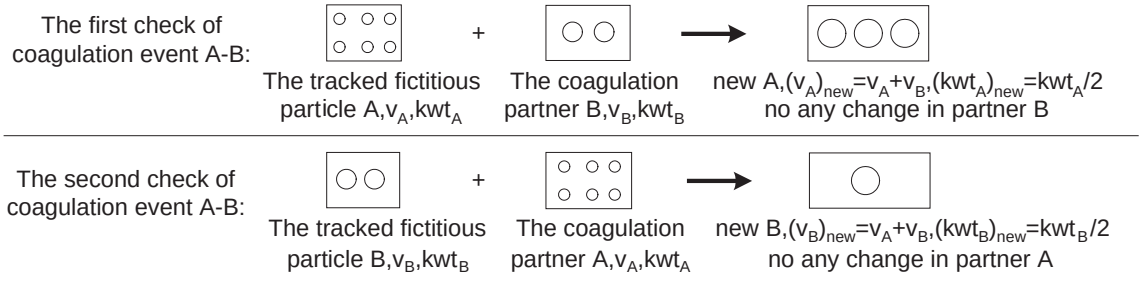

Fig. 5. Schematic diagram of the consequential treatment of coagulation event.

Table 1
The list of computation conditions and corresponding computation cost

Condition	Case	C	B	τ_C (s)	τ_B (s)	N_0	N_f	v_0 (or v_{g0}) (μm^{-3})	Evolution time (s)	CPU time (s)
1	Case 1	2×10^{-9}	0.005	50	200	10^7	3000	1	5000	492
2	Case 1	10^{-8}	0.005	10	200	10^7	3000	1	1000	240
3	Case 1	10^{-7}	0.005	1	200	10^7	3000	1	100	110
4	Case 2	10^{-7}	10	1	0.1	10^7	3000	1	4	570
5	Case 2	10^{-7}	0.5	1	2	10^7	3000	1	80	630
6	Case 2	10^{-7}	0.25	1	4	10^7	3000	1	160	628
7	Case 3	10^{-7}	10	1	0.1	10^7	3000	1	4	572
8	Case 3	10^{-7}	0.5	1	2	10^7	3000	1	80	616
9	Case 3	10^{-7}	0.25	1	4	10^7	3000	1	160	629
10	Case 4	6.405×10^{-10}	0.011	1561.28	3122.56	10^6	3000	0.029	1561.28	74

when the random number R_2 becomes smaller than the breakage probability of i within Δt, i.e.,

$$R_2 \le S_i \times \Delta t. \tag{19}$$

The fragment from breakage of fictitious particle i is described by fragment size distribution. γ_{ij} is probability of making a fragment of index j from a parent of index i, b_i is total number of particles resulting from the breakage of a particle of index i. The constraints on γ_{ij} and b_i is [4,5,30]:

(i) $\sum_j \gamma_{ij} = 1$, which indicates that every fragment will be considered.
(ii) $b_i \ge 2$, which shows that the total number of fragments is greater than or equal to 2, even infinite.
(iii) $\sum_j v_j \gamma_{ij} b_i = v_i$, which indicates the mass of parent particle is equal to the total mass of fragments.

If fictitious particle A (index i, transform-weight kwt_A) has affirmed to break up, the first step is to get the total number of fragments according to b_i. And then fragment size distribution is gained according to both γ_{ij} and b_i. As far as one binary breakage event is considered, ones assume two fragments are fictitious particle B and C, respectively (corresponding index j and k, transform-weight kwt_B and kwt_C, respectively). Based on the law of conservation of mass and the rule of number of fragments, two fragments can be described as follows:

$$kwt_A = kwt_B = kwt_C; v_A = v_B + v_C. \tag{20}$$

When the size of one fragment j is decided according to γ_{ij}, the size of the other fragment k is decided according to Eq. (20).

Attentively, the sum of fictitious particles will be added one at least along with one breakage event unless measures are adopted. One of important points of treating breakage event is to keep the total number of fictitious particles constant. Some measures are adopted as follows: the first fragment is stored in the position of the parent particle i and other fragments are merged, respectively, with one fictitious particle that has same or similar size with the

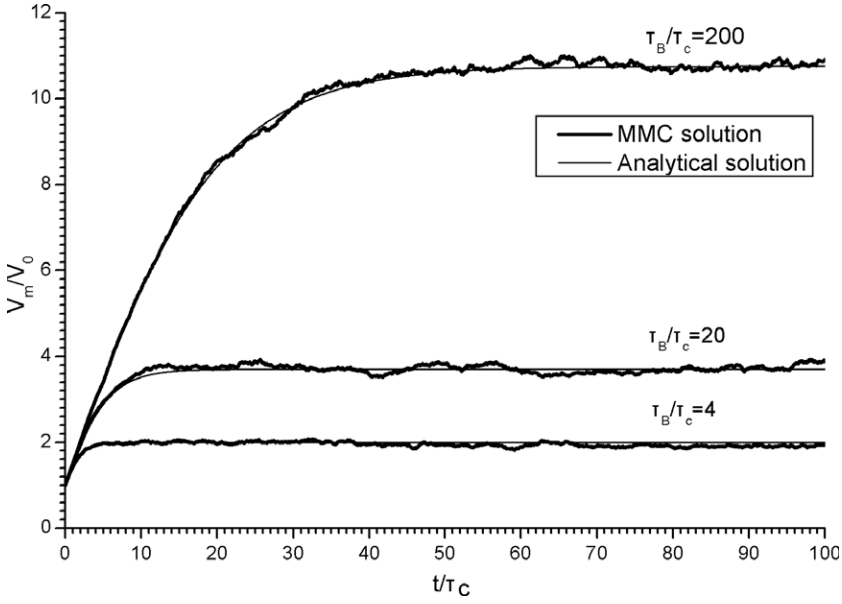

Fig. 6. Evolution of the particle ratio average size as a function of time for Case 1.

fragment. As for a binary breakage, the law of mergence is as follows:

$$(v_D)_{\text{new}} = v_D; (\text{kwt}_D)_{\text{new}} = \text{kwt}_D + \text{kwt}_C \quad (21)$$

where fictitious particle C is the other fragment. Fictitious particle C is merged with fictitious particle D, which is chosen randomly from fictitious particle array. Before merging the volume of C and D is v_C and v_D ($v_D \approx v_C$), and the transform-weight is kwt_C and kwt_D, respectively. After merging, the volume and transform-weight of D are $(v_D)_{\text{new}}$ and $(\text{kwt}_D)_{\text{new}}$ respectively and are updated.

Those measures will conserve the total number of fictitious particles.

3. Algorithm validation

To validate MMC method for GDE considering simultaneous coagulation and breakage, four cases in which complete or partial analytical solutions exist are chosen and simulated numerically. All cases are binary coagulation and binary breakage ($b_i=2$). In Case 1~3 initial particle size distribution is monodisperse, initial number, N_0, and initial size, v_0. In the paper, we choose $v_0=1$ μm^3, $N_0=10^7$ particles/cm^3 for Case 1~3. In Case 4, initial particle size distribution is polydisperse and is represented by an exponential function:

$$n_p(v,0) = \frac{N_0}{v_{g0}} e^{-\frac{v}{v_{g0}}} \quad (22)$$

where v_{g0} is initial mean geometric size. In Case 4 we choose $N_0=10^6$ particles/cm^3, $v_{g0}=0.029$ μm^3. In addition we choose the total number of fictitious particles $N_f=3000$ when simulating Case 1~4.

3.1. Case 1

This is a discrete model in which primary particles (or monomers) coagulate to form larger clusters, which in turn break into pieces containing a discrete number of primaries. Coagulation kernel β is constant number C, which is independent of particle size. The characteristic coagulation time is defined as $\tau_C=1/(CN_0)$. Only those particles which size is greater than that of the primary particle could break up and the smallest fragment size is v_0. Breakage rate S is proportional to the number of primary particles in the cluster, that is, $S=B(p_n-1)$, where B is constant number and $p_n=v/v_0$ is the number of primary particles in the cluster of volume v. As for primary particles, $p_n=1$, $S=0$. The characteristic breakage time is defined as $\tau_B=1/B$. Numerical values of kernels and time scales are gathered in Table 1. The distribution of fragments is uniform, i.e., fragments of any size appear with equal probability. The probability γ_{ij}, that a parent particle containing i primary particles will generate a daughter particle containing j primary particles is [10]:

$$\gamma_{ij} = \begin{cases} 1/(p_{ni}-1) & p_{ni} > 1 \text{ and } 1 \le p_{nj} \le p_{ni}-1 \\ 0 & \text{otherwise} \end{cases}. \quad (23)$$

Assuming R_3 is a random number uniformly distributed between 0 and 1, the size of fragment j is calculated as follows [10]:

$$v_j = v_0\{\text{integer}[R_3(p_{ni}-1)]+1\} \quad (24)$$

where integer [] indicates the integer part of its argument. The size of the other fragment is $v_k=v_i-v_j$.

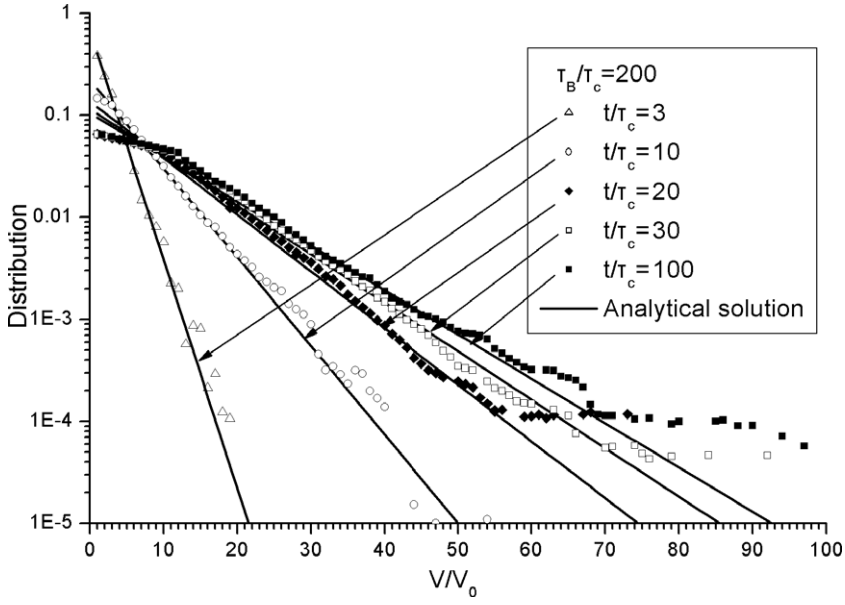

Fig. 7. Particle size distributions at some time-point with $\tau_B/\tau_C=200$ for Case 1.

The ratio of the average steady-state size to initial average size (called ratio average size) is obtained [10]

$$v_{m,\infty} = \frac{V_{m,\infty}}{V_{m,0}} = \frac{N_0}{N_\infty} = \frac{1+\sqrt{1+2\tau_B/\tau_C}}{2}. \quad (25)$$

The time evolution of the ratio average size is [4]:

$$v_m(t) = \frac{V_m(t)}{V_{m,0}} = \frac{N_0}{N(t)} = 1 + \frac{2V_{m,\infty}(v_{m,\infty}-1)}{1+(2v_{m,\infty}-1)c\mathrm{th}\left[\frac{t}{\tau_B}(v_{m,\infty}-1/2)\right]}. \quad (26)$$

where cth() indicates hyperbolic cotangent function.

Analytical solution of particle size distribution n_i is as follows [10]:

$$n_i(t) = \frac{N_i}{N(t)} = \frac{1}{v_m(t)-1}\left(1-\frac{1}{v_m(t)}\right)^{p_{ni}} \quad (27)$$

$n_i(t)$ represents the radio of the number of particles containing i primary particles to the total number of all particles at time t. It is apparent that $\sum_i n_i = \sum_i N_i/N(t) = 1$. In addition, the normalized size distribution is $n(v)=n_i(t)/v$.

The ratio average size as a function of time is shown in Fig. 6. Since primary particles do not break up, the average size will only increase in the discrete cases. Along with the evolution of time the average size increases and the total

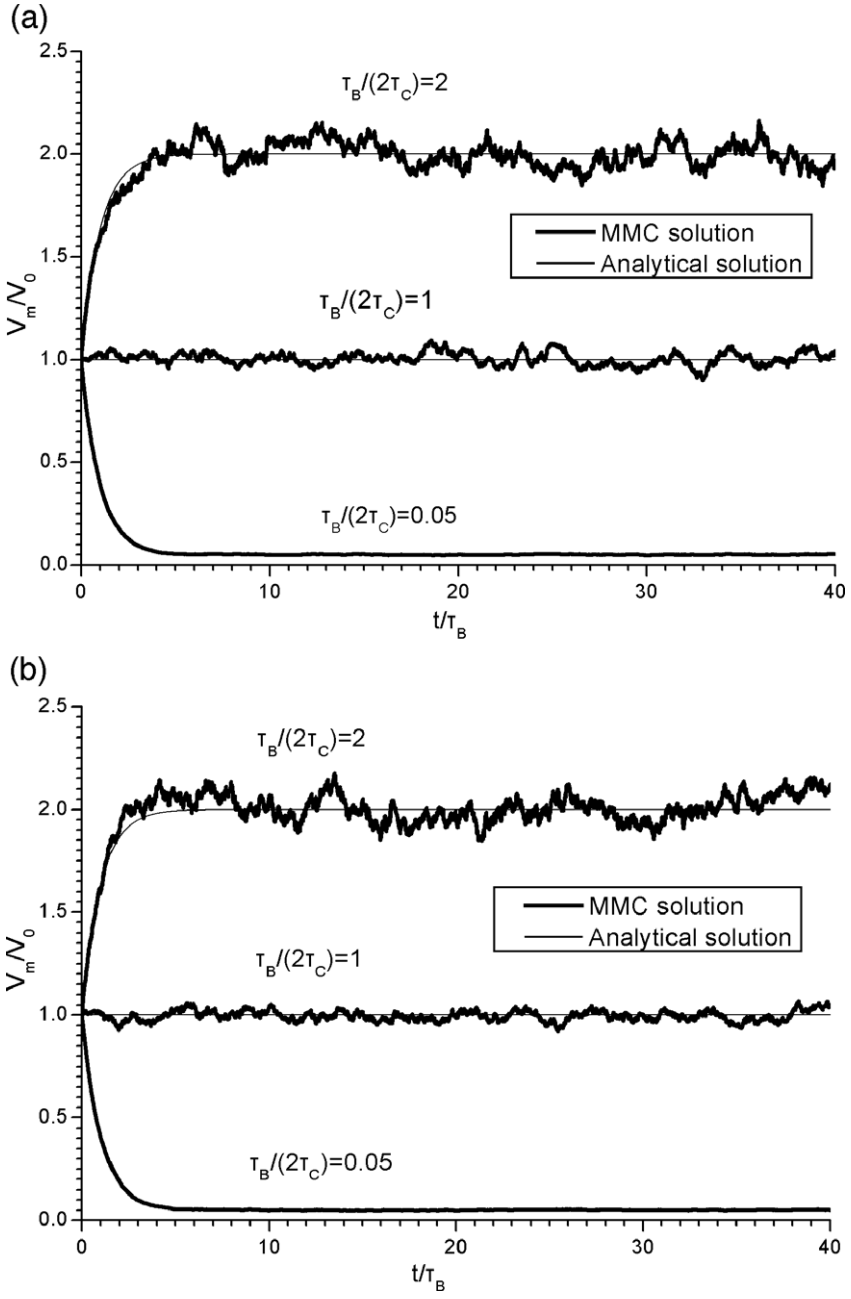

Fig. 8. Evolution of the particle ratio average size as a function of time for (a) Case 2; (b) Case 3.

number of real particles decreases, which indicates coagulation "defeats" breakage. However the average size and the total number of real particles will get to a steady-state condition further, which indicates coagulation equalizes breakage. By setting various ratio of coagulation kernel constant C to breakage rate constant B, the steady-state ratio average size can be adjusted arbitrarily, but at least greater than 1. The simulation result of MMC method for GDE agrees with analytical solution on the whole.

Fig. 7 illustrates particle size distribution at various times with $\tau_B/\tau_C=200$ for Case 1. The simulation results make clear that the exponential form of PSD is approached even as early as $t=3\tau_C$ and is hold until steady state (such as $t=100\tau_C$). On the lower end and upper end of particle size distribution, the agreement between MMC solution and analytical solution is bad, although it is still good qualitatively. It is noticeable that the initial number of real particles is 10^7 while the total number of fictitious particles is only 3000, i.e., one fictitious particle represents about 3333 real particles. If increasing the number of fictitious particles, one can foresee higher computation precision, however at the cost of increasing computation cost. The other possible reason of numerical bias may originate from a discrete binning method that is used to get size distribution. Size distribution is divided into bins by certain kinds of law between the smallest and largest size, and the number of particles in each bin is counted and converted into PSD. Furthermore the floating-point operational precision of

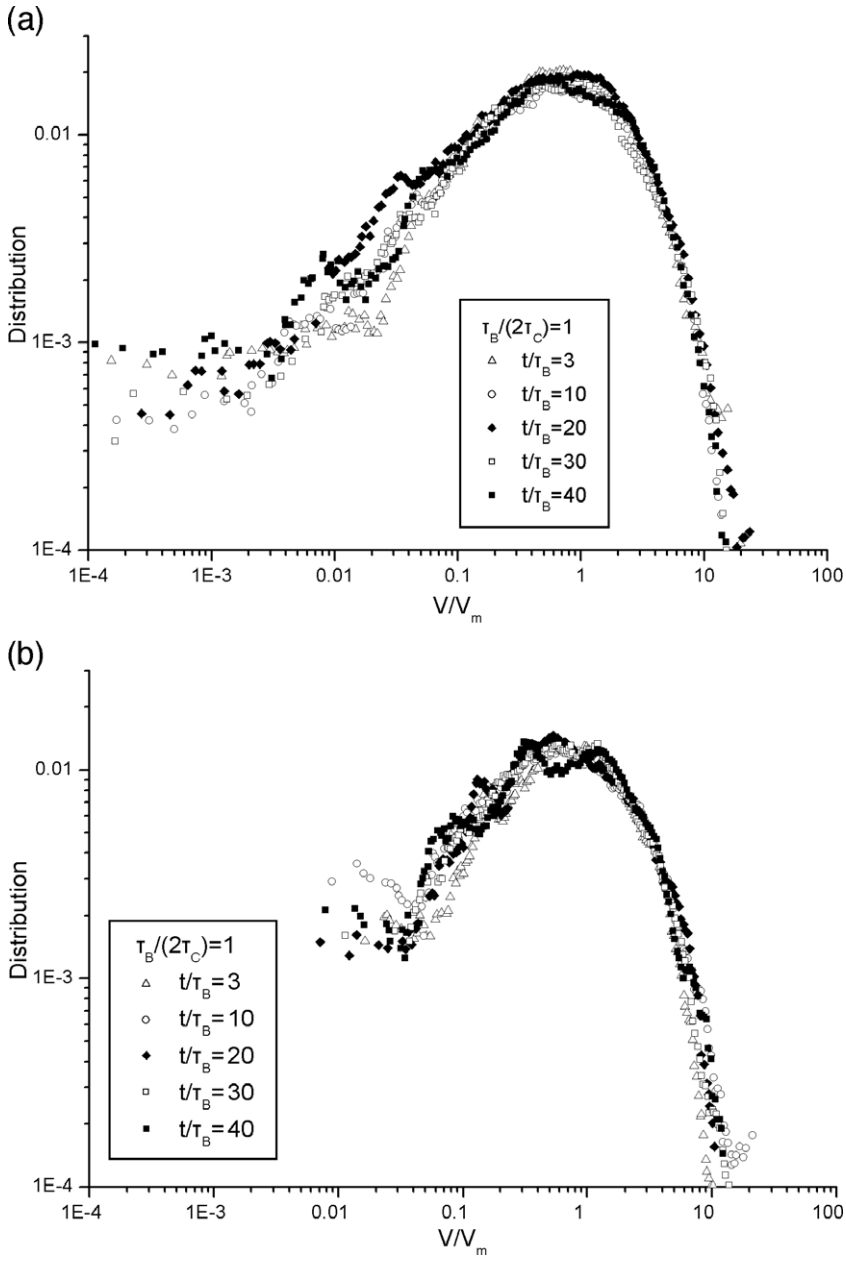

Fig. 9. Particle size distributions at some time-point with $\tau_B/2\tau_C=1$ for (a) Case 2; (b) Case 3.

computer may contribute partly to the numerical bias on the upper end of PSD, in which the values of distribution n_i reach to the magnitude of 10^{-8}. Because the number of those particles on the upper end of PSD is small, the numerical result of MMC method is still satisfying.

3.2. Case 2 and Case 3

The two cases are continuous model. Coagulation kernel β is still constant number C, and breakage rate S is constant number B independent of size. Comparing with Case 1, every particle including primary particle has possibility of breakage. The difference of the two cases lies in: the fragment distribution in Case 2 is uniform and in Case 3 equal-size. If R_4 is a random number uniformly distributed between 0 and 1, the size of one fragment for Case 2 is $v_j=R_4 v_i$ and the size of other fragment is $v_k=(1-R_4)v_i$; the size of two fragment for Case 3 is $v_j=v_k=0.5v_i$.

Analytical solution of steady-state ratio average size for both Case 2 and Case 3 is given by Lee and Matsoukas [10]:

$$v_{m,\infty}=\frac{V_{m,\infty}}{V_{m,0}}=\frac{N_0}{N_\infty}=\frac{\tau_B}{2\tau_C}. \tag{28}$$

And the time evolution of the ratio average size is as follows [10]:

$$v_m(t)=\frac{V_m(t)}{V_{m,0}}=\frac{N_0}{N(t)}=1+\left(1-v_{m,\infty}\right)\exp\left(-\frac{t}{\tau_B}\right). \tag{29}$$

Fig. 8 shows the time evolution of the ratio average size for Case 2 and Case 3. Since the size of fragment is continuously distributed, the average size can increase or decrease according to the various ratio τ_B/τ_C or B/C. Along with time evolution, the average size and the total number get to steady state, which indicates coagulation and breakage is in the state of equilibrium. The simulation results of MMC method for GDE agree with analytical solutions well.

Fig. 9 shows particle size distribution at various times with $\tau_B/\tau_C=1$ for Case 2 and Case 3. The particle size distribution remains basically the exponential distribution from a short evolution time ($t=3\tau_B$) to a long evolution time ($t=40\tau_B$), which is "self-preserving" curve [31]. When particle size is small ($V/V_m \ll 1$ in Fig. 9), the plotted distribution scattered seriously. In the same way, the source of numerical deviations is the limited number of fictitious particles, the discrete binning method and the floating-point operational precision of computer. Here the number of bins is 200, logarithmically spaced.

Fig. 10 shows steady-state normalized size distribution with $\tau_B/2\tau_C=1$ for Case 2 and Case 3. The average size remains constant through the simulation, so does the particle number. The size distribution is independent of time. The results in Fig. 10 come from those at time $t=40\tau_B$. For $V/V_m \ll 1$, Diemer [32] and Diemer and Olson [33] have obtained asymptotic expressions of the steady-state normalized size distribution, which is drawn as two lines with slope $-2/3$ for Case 2 and slope -0.415 for Case 3. MMC solution agrees with asymptotic expressions qualitatively.

Fig. 11 shows the collapse speed rate of the average size. The numerical result can be compared with analytical solution of Eq. (29). The agreement is good on the whole, however it becomes worse along with the time evolution. The source of numerical bias is the same with the above analysis.

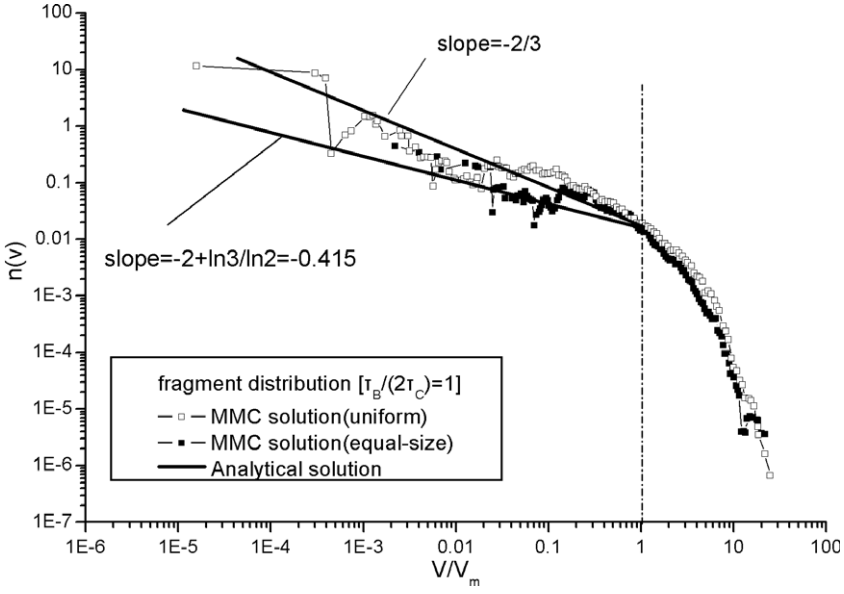

Fig. 10. Normalized particle size distribution for Case 2 and Case 3 with steady-state ($\tau_B/2\tau_C=1$).

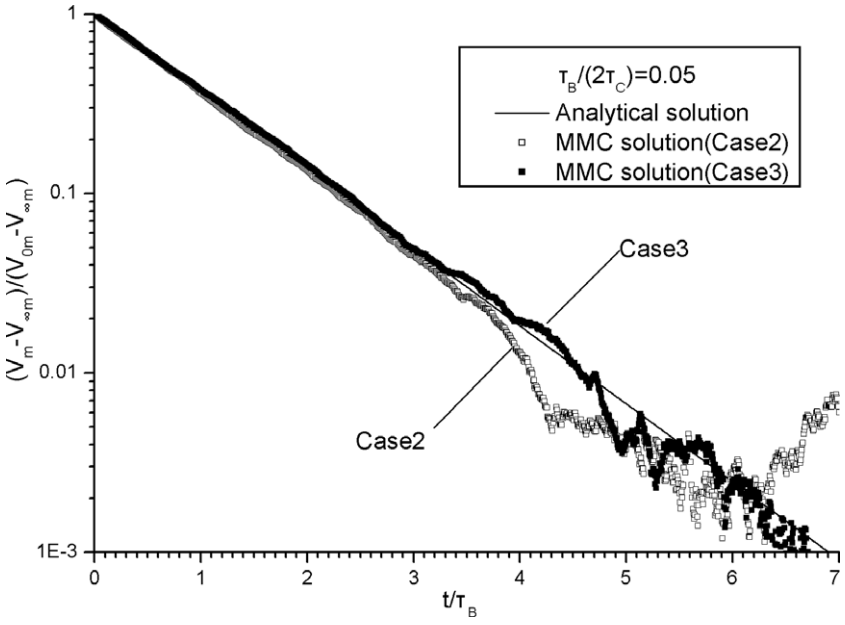

Fig. 11. Collapse rate of the particle average size for Case 2 and Case 3 with $\tau_B/2\tau_C=0.05$.

3.3. Case 4

In fact Case 4 is the Baltz–Tobolsky problem (Case 1) in continuous spectrum form, which is solved by Patil and Andrews [34] using the Laplace transform on the particle size variable. Case 4 is analogous to simultaneous coagulation and breakage with constant coagulation kernel, first-order breakage rate and binary uniform fragment size distribution. Here $\gamma(u,v)=1/v$, $b(u)=2$, $S(u)=Bu$, $\beta(v,u)=C$ corresponding to Eq. (1). It can be proved that the total number of particles is constant by choosing the values of the problem parameters to satisfy $B=2v_{g0}/C$ [34]. In the condition particle size distribution conserves steady state at any time, so the initial PSD, Eq. (22), is also the equilibrium solution.

Fig. 12 shows particle size distribution at various times for Case 4. The exponential form particle size distribution is conserved basically at those time points. Fig. 13 shows the total number of particles with the evolution of time. Here the number of discrete bins is 200, logarithmically spaced.

Computation costs for various conditions of those cases are listed in Table 1. Hardware and software environment are as follows: Athlon Xp2500+, 512M, Visual Fortran 6.0, Windows Xp professional. There are only several hundreds seconds for any computational condition. Thus the low

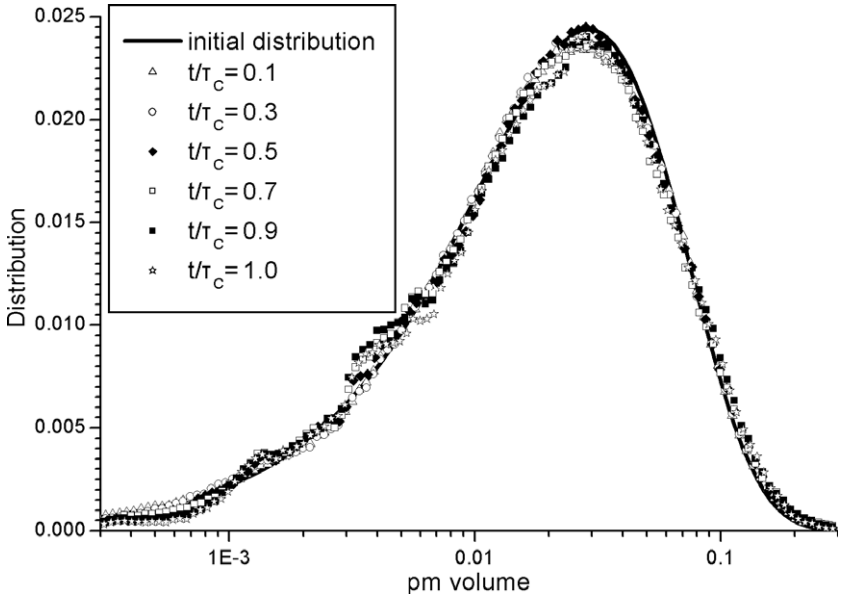

Fig. 12. Particle size distributions at some time-point for Case 4.

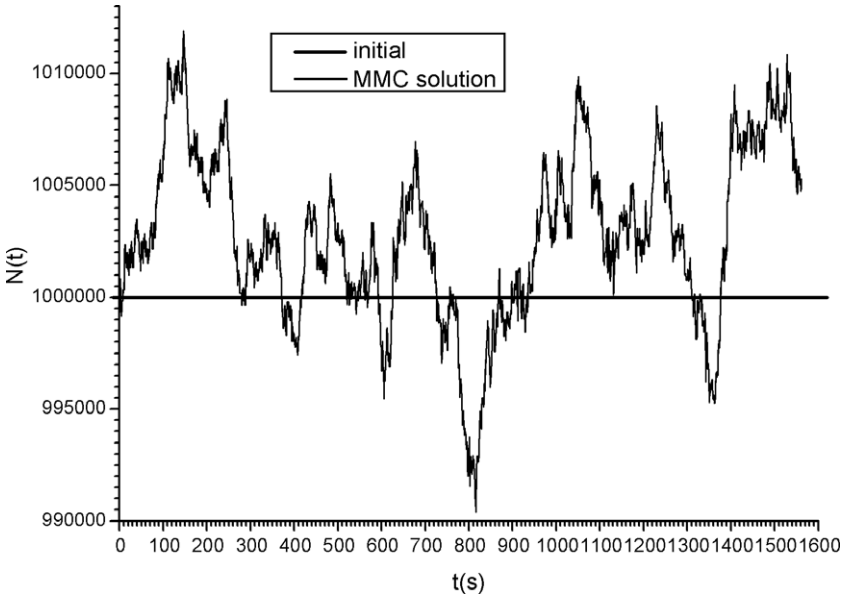

Fig. 13. The total number of particles with the evolution of time.

computation cost of MMC method will encourage its engineering computation.

4. Conclusion

Multi-Monte Carlo (MMC) method solving general dynamic equation (GDE) for simultaneous coagulation and breakage is performed in the paper. The paper has described in detail the MMC method. Its characteristics are as follows: the introduction of the concept of weighted fictitious particles, constant number of fictitious particles, and constant computational domain. MMC method is the combination of "time-driven" MC, constant number method and constant volume method. The other remarkable advantage of MMC method is its good expansibility. Since MMC method has the possibility of discarding the concept of "subsystem", MMC method has possibility to account for space dispersion of particle size function, boundary conditions and particle Lagrangian tracking, etc, although the paper does not realize numerically the possibility, which will be developed in the next stage.

MMC method has been used to simulation four special cases. The agreement between MMC solution and analytical solution is mostly good, which validated high and stable computation precision of MMC method. Furthermore computation cost of MMC method is low enough to apply engineering computation and general scientific quantitative analysis.

Notations

$b(u)$, b_i	The number of fragments resulting from the breakage of a particle of volume u (index i)
B	Constant number
C_i	Coagulation probability of fictitious particle i
C	Constant number
kwt	Transform-weight of fictitious particle
n	The radio of the number of particles
n_p	Particle size distribution density function, particles/m^3/m^3
nc	The average coagulation event of each real particle per unit time
N	The total number of particles
NC	The number of coagulation events
P_{ij}	The probability of particle i coagulating with any other fictitious particles j
p_n	The number of primary particles
R_1, R_2, R_3, R_4	Random number from a uniform distribution in the interval [0,1]
S	Constant breakage rate, s^{-1}
$S(v)$,S_i	The breakage rate for particle of volume v (index i), s^{-1}
t	Time, s
u,v	The volume of particle, m^3
v	Ratio average size
V	Control volume, m^3
V	The volume of particle, m^3

Greek letters

α	Multiplicative constant
β	Coagulation kernel, m^3/particles/s
$\gamma(u,v)$, γ_{ij}	The probability of making a daughter of volume v (index j) from a parent of volume u (index i)
τ	The characteristic time scale, s
Δt	Time step, s

Subscripts

0	Refers to initial condition
∞	Refers to condition at $t \to \infty$
A, B, C, D	Refers to the index of fictitious particle

coag, C Refers to coagulation
brk, B Refers to breakage
f Refers to fictitious particle
g Refers to geometric mean value
m Refers to mean value
i, j, k Refers to the index of fictitious particle
min Refers to minimum value
max Refers to maximum value
new Refers to the condition after coagulation event or breakage event
p Refers to particle phase

Acknowledgements

We wish to thank "National Key Basic Research and Development Program 2002CB211602" and "the National Natural Science Foundation of China under grant number 90410017" for funds.

References

[1] W.S. Seames, An initial study of the fine fragmentation fly ash particle mode generated during pulverized coal combustion, Fuel Processing Technology 81 (2003) 109–125.
[2] W.G. Tucker, An overview of PM2.5 sources and control strategies, Fuel Processing Technology 65–66 (2000) 379–392.
[3] Z. Meng, D. Dabdub, J.H. Seinfeld, Size-resolved and chemically resolved model of atmospheric aerosol dynamic, Journal of Geophysical Research 103 (1998) 3419–3435.
[4] P.J. Blatz, A.V. Tobolsky, Note on the kinetics of systems manifesting simultaneous polymerization–depolymerization phenomena, Journal of Physical Chemistry 49 (1945) 77–79.
[5] R.B. Diemer, J.H. Olson, A moment methodology for coagulation and breakage problems: Part 1. Analytical solution of the steady-state population balance, Chemical Engineering Science 57 (2002) 2193–2209.
[6] B.K. Mishra, Monte Carlo simulation of particle breakage process during grinding, Powder Technology 110 (2000) 246–252.
[7] Parichay K. Das, Monte Carlo simulation of drop breakage on the basis of drop volume, Computers & Chemical Engineering 20 (3) (1996) 307–313.
[8] M. Balmelli, L. Steiner, Monte Carlo simulation of drop dispersion behavior, Chemical Engineering and Processing 39 (2000) 201–206.
[9] M. Kostoglou, S. Dovas, A.J. Karabelas, On the steady-state size distribution of dispersions in breakage processes, Chemical Engineering Science 52 (8) (1997) 1285–1299.
[10] K. Lee, T. Matsoukas, Simultaneous coagulation and breakage using constant-N Monte Carlo, Powder Technology 110 (2000) 82–89.
[11] M. Smith, T. Matsoukas, Constant-number Monte Carlo simulation of population balance, Chemical Engineering Science 53 (9) (1998) 1777–1786.
[12] Y. Lin, K. Lee, T. Matsoukas, Solution of the population balance equation using constant-number Monte Carlo, Chemical Engineering Science 57 (2002) 2241–2252.
[13] F.E. Kruis, A. Maisels, H. Fissan, Direct simulation Monte Carlo method for particle coagulation and aggregation, AICHE Journal 46 (9) (2000) 1735–1742.
[14] M. Vanni, Approximate population balance equations for aggregation-breakage processes, Journal of Colloid and Interface Science 221 (2000) 143–160.
[15] J.D. Landgrebe, S.E. Pratsinis, Gas-phase manufacture of particulate: interplay of chemical reaction and aerosol coagulation in the free-molecular regime, Industrial & Engineering Chemistry Research 28 (1989) 1474–1481.
[16] J.J. Wu, R.C. Flagan, A discrete–sectional solution to the aerosol dynamic equation, Journal of Colloid and Interface Science 123 (1988) 339–352.
[17] K. Liffman, A direct simulation Monte-Carlo method for cluster coagulation, Journal of Computational Physics 100 (1992) 116–127.
[18] A.L. Garcia, A Monte Carlo simulation of coagulation, Physica 143A (1987) 535–546.
[19] K.K. Sabelfeld, S.V. Rogansinsky, A.A. Kolodko, et al., Stochastic algorithms for solving Smoluchovsky coagulation equation and applications to aerosol growth simulation, Monte Carlo Methods and Applications 2 (1) (1996) 41–87.
[20] A. Eibeck, W. Wagner, Approximative solution of the coagulation-fragmentation equation by stochastic particle systems, Stochastic Analysis and Applications 18 (6) (2000) 921–948.
[21] A. Eibeck, W. Wagner, An efficient stochastic algorithm for studying coagulation dynamics and gelation phenomena, SIAM Journal on Scientific Computing 22 (3) (2000) 802–821.
[22] A. Eibeck, W. Wagner, Stochastic particle approximations for Smoluchowski's coagulation equation, Annals of Applied Probability 11 (4) (2001) 1137–1165.
[23] B. Jourdain, Nonlinear processes associated with the discrete Smoluchowski coagulation fragmentation equation, Markov Processes and Related Fields 9 (1) (2003) 103–130.
[24] E. Debry, B. Sportisse, B. Jourdain, A stochastic approach for the numerical simulation of the general dynamics equation for aerosols, Journal of Computational Physics 184 (2003) 649–669.
[25] M. Goodson, M. Kraft, Simulation of coalescence and breakage: an assessment of two stochastic methods suitable for simulating liquid–liquid extraction, Chemical Engineering Science 59 (2004) 3865–3881.
[26] H.B. Zhao, C.G. Zheng, M.H. Xu, Multi-Monte Carlo Method for Particle Coagulation: Description and Validation, Applied Mathematics and Computation 26 (7) (2005) 875–882.
[27] H.B. Zhao, C.G. Zheng, M.H. Xu, Multi-Monte Carlo method for coagulation and condensation/evaporation in dispersed systems, Journal of Colloid and Interface Science 286 (2005) 195–208.
[28] K.C. Hu, R. Mei, Particle collision rate in fluid flows, Physics of Fluids 10 (4) (1998) 1028–1030.
[29] K. Nanbu, Direct simulation scheme derived from the Boltzmann equation: I. Monocomponent gases, Journal of the Physical Society of Japan 49 (1980) 2042–2049.
[30] D.P. Patil, J.R.G. Andrews, An analytical solution to continuous population balance model describing floc coalescence and breakage—a special case, Chemical Engineering Science 53 (3) (1998) 599–601.
[31] S.K. Friedlander, C.S. Wang, The self-preserving particle size distribution for coagulation by Brownian motion, Journal of Colloid and Interface Science 22 (1966) 126–132.
[32] R.B. Diemer, Moment Methods for Coagulation, Breakage and Coalescence Problems, PhD thesis, University Delaware, 1999.
[33] R.B. Diemer, J.H. Olson, Basis functions for inversion of moment problems, Advanced Technologies for Particle Production, Proceedings of Particle Technology Forum Topical Conference at 1998 Annual Meeting, AIChE, 1998, p. 99.
[34] D.P. Patil, J.R.G. Andrews, An analytical solution to continuous population balance model describing floc coalescence and breakage—a special case, Chemical Engineering Science 53 (3) (1998) 599–601.